Published in final edited form as:
Abdom Imaging. 2015 January ; 40(1): 207–221. doi:10.1007/s00261-014-0178-x.

Prospective Evaluation of Prior Image Constrained Compressed Sensing (PICCS) Algorithm in Abdominal CT: A comparison of reduced dose with standard dose imaging

Meghan G. Lubner, MD[1], **Perry J. Pickhardt, MD**[1], **David H. Kim, MD**[1], **Jie Tang, PhD**[2], **Alejandro Munoz del Rio, PhD**[1], and **Guang-Hong Chen, PhD**[1,2]

[1]department of Radiology, University of Wisconsin School of Medicine and Public Health, Madison, WI

[2]Medical Physics, University of Wisconsin School of Medicine and Public Health, Madison, WI

Abstract

Purpose—To prospectively study CT dose reduction using the "prior image constrained compressed sensing" (PICCS) reconstruction technique.

Methods—Immediately following routine standard dose (SD) abdominal MDCT, 50 patients (mean age, 57.7 years; mean BMI, 28.8) underwent a second reduced-dose (RD) scan (targeted dose reduction, 70-90%). DLP, $CTDI_{vol}$ and SSDE were compared. Several reconstruction algorithms (FBP, ASIR, and PICCS) were applied to the RD series. SD images with FBP served as reference standard. Two blinded readers evaluated each series for subjective image quality and focal lesion detection.

Results—Mean DLP, $CTDI_{vol}$, and SSDE for RD series was 140.3 mGy*cm (median 79.4), 3.7 mGy (median 1.8), and 4.2 mGy (median 2.3) compared with 493.7 mGy*cm (median 345.8), 12.9 mGy (median 7.9 mGy) and 14.6 mGy (median 10.1) for SD series, respectively. Mean effective patient diameter was 30.1 cm (median 30), which translates to a mean SSDE reduction of 72% ($p<0.001$). RD-PICCS image quality score was 2.8±0.5, improved over the RD-FBP (1.7±0.7) and RD-ASIR(1.9±0.8)($p<0.001$), but lower than SD (3.5±0.5)($p<0.001$). Readers detected 81% (184/228) of focal lesions on RD-PICCS series, versus 67% (153/228) and 65% (149/228) for RD-FBP and RD-ASIR, respectively. Mean image noise was significantly reduced on RD-PICCS series (13.9 HU) compared with RD-FBP (57.2) and RD-ASIR (44.1) ($p<0.001$).

Conclusion—PICCS allows for marked dose reduction at abdominal CT with improved image quality and diagnostic performance over reduced-dose FBP and ASIR. Further study is needed to determine indication-specific dose reduction levels that preserve acceptable diagnostic accuracy relative to higher-dose protocols.

Keywords

CT; Dose Reduction; Iterative Reconstruction

Corresponding Author: Meghan G. Lubner, MD, Department of Radiology, University of Wisconsin School of, Medicine and Public Health, E3/311 Clinical Sciences Center, 600 Highland Ave, Madison, WI 53792-3252, mlubner@uwhealth.org, Ph: 608-263-9028 Fax: 608-263-0140.

Introduction

The clinical usage of CT has continued to expand, making dose reduction, particularly in more vulnerable patient populations, a top priority (1-4). The small theoretical risk associated with ionizing radiation has led to increasing concern on the part of both patients and referring physicians, which has in turn, led to the emergence of a variety of dose reduction strategies including tube current modulation (5-9), automated exposure control (10-13), voltage adjustment based on patient size (14) and use of alternative image reconstruction methods (15-23). Adaptive statistical iterative reconstruction (ASIR) (ASiR, GE Healthcare, Waukesha WI), has shown dose reduction potential, in the 25-40% range (17, 24-26) and can be performed nearly instantaneously at the time of image acquisition. The more computationally intense model based iterative reconstruction (MBIR) techniques (Veo, GE Healthcare, Waukesha WI) may allow for more aggressive dose reduction, on the order of 70% (21). Despite these dose savings, a drawback of commercially available model based techniques is that they can be time consuming, with reconstruction times ranging from 30 minutes to over 2 hours.

The challenge of reducing dose involves a balance between the image quality necessary for a specific diagnostic task and the targeted level of dose reduction. For any emerging radiation dose reduction technique, it would be highly desirable to study the needed radiation dose level for a clinical diagnostic task (27). The purpose of this paper is to prospectively investigate the dose reduction potential for another iterative reconstruction algorithm referred to as prior image constrained compressed sensing (PICCS) (20). This technique was retrospectively studied in the abdomen and pelvis and showed promise for substantial dose savings (28). The preliminary results using PICCS for dose reduction, initially targeted at 70-90%, are reported in this paper as part of an ongoing prospective clinical trial.

Subjects and Methods

Study population and scanning

This HIPAA-compliant prospective study was approved by the institutional review board at our institution. All subjects provided signed informed consent. Eligible patients included adult men and non pregnant women scheduled to undergo supine contrast enhanced or unenhanced CT of the abdomen and pelvis as part of their routine clinical care. Study dates ranged from 3/29/2011-2/4/20912. All patients were scanned on a 64-slice multidetector CT (MDCT) scanner, (Discovery 750 HD, GE Medical, Waukesha WI). Scan parameters included a collimated slice thickness at the isocenter of 0.625 mm, 120 kVp, tube current modulation (Smart mA, GE Healthcare) and a study specific noise index ranging up to 50 for the standard dose (SD) series (slice thickness for noise index 1.25 mm, smart mA range 30-660 depending on indication, see Appendix 1). We selected our noise indices by first performing a phantom study looking at noise level changes and low contrast lesion detection at varying radiation doses with and without PICCS reconstruction, followed by retrospective review of noise reduction and image quality in clinical protocols (28). We used this data to target dose levels of 20-30% of our clinical scans for our reduced dose scans. Therefore, we

adjusted the NI of the clinical protocol up to reduce the dose 20-30%, enabling us to perform one additional reduced dose scan at 20-30% the baseline clinical dose prescription at a net equal dose to our routine clinical scans.

For each patient, the routine clinical exam with standard protocol at our institution was initially performed. Immediately following this series, a second dose-modified scan (targeted dose reduction in range of 70-90%) was added based on the projected dose-length product of the clinical dose scan. On non contrast studies for screening or for urolithiasis, the dose reduction was pushed lower, whereas dose reduction for contrast enhanced scans looking for low contrast lesions, dose reduction was more conservative in the 70% range. The noise index and tube current range were adjusted to achieve the targeted dose reduction. For IV-contrast enhanced studies, the reduced dose exam was obtained in the same breath hold to minimize differences in the phase of contrast (standard portal venous phase, obtained approximately 70 seconds after contrast injection). Patients were not re-injected with contrast. The study cohort was comprised of 50 adult subjects (23 females, 27 males; mean age, 57.7 years) included a cohort of 24 non-contrast and 26 post-contrast CT examinations. Of the 24 non contrast studies, 11 were performed for screening CT colonography, and 13 were performed for flank pain looking for urolithiasis. The contrast enhanced CTs were largely performed for oncologic follow up. No patient that was scanned under this protocol was subsequently excluded. The mean patient body mass index (BMI) was 28.8 (range 19.4-43.4). 19 subjects (38%) were obese (BMI>30) (Table 1).

Radiation Dose Metrics

The volume CTDI index ($CTDI_{vol}$, mGy) and dose-length product (DLP, mGy*cm) were recorded for the matching standard dose and reduced dose series. In addition, effective dose (mSv) was obtained from the dose-length product using the conversion factor 0.015 mSv/(mGy*cm) recommended by the American Association of Physicists in Medicine (29) and verified by Deak et al (30). The recently recommended size specific dose estimate (SSDE) (31, 32) was also generated as follows. All slices from a CT volume were collapsed into a thick slice along the z axis (Figure 1). The lateral and AP dimensions were measured on the −400 HU outline of the thick slice and were used as the average lateral and AP dimensions of the volume. An effective diameter was obtained by taking the square root of the product of the average lateral width and AP diameter. This effective diameter allowed the selection of a conversion factor based on the use of a 32 cm phantom to be multiplied by $CTDI_{vol}$ to get a size specific dose estimate (SSDE) (31, 32). The SSDE takes into account the individual patient size when assessing dose.

CT Image Reconstruction

The standard dose abdominal CT was reconstructed using filtered back projection (FBP). The reduced dose series was reconstructed using several techniques including FBP, ASIR (GE Healthcare, Waukesha, WI), and PICCS, an iterative reconstruction technique developed at the authors' institution. For the ASIR series, a 40% blend was applied, as previously described for optimal image quality (17, 24, 33). PICCS was applied to reconstruct images using a standard PC (Dual Intel Xeon 2.33 GHz CPUs, 8G Ram) with an NVidia GeForce GTX 295 graphic card (480 CUDA cores). With PICCS, the FBP images

for all series are forward-projected to generate synthesized projection data and low-pass filtered to generate a new image series with lower noise and lower spatial resolution image than the original FBP images. The generated low noise, low spatial resolution images represent the 'prior image' in the PICCS algorithm used to reconstruct the final image series from the synthesized projection data (34). In PICCS image reconstruction, the noise level of the final image is primarily determined by the prior image while the spatial resolution in the final image is determined by the projection data. Using the PICCS reconstruction algorithm, the traditional tradeoff between noise level and spatial resolution is decoupled to achieve both low noise and high spatial resolution CT reconstruction as described previously (20, 28). All images (standard and reduced dose) were reconstructed with 1.25 mm slice thickness at 0.625 mm intervals in the transverse plane. Images were later reformatted into both the transverse and coronal planes with 2.5 mm slice thickness at 1.25 mm intervals, which were used for clinical assessment (Figure 2). Given that an assessment of the effect on PICCS on spatial resolution was previously performed in a retrospective review (28), that assessment was not repeated here.

CT Image Analysis

The CT images were evaluated for image noise, subjective image quality, and lesion detection. Objective CT image noise was recorded as the standard deviation of the attenuation (HU) using a 250 mm^2 region of interest (ROI) placed in four standard locations including the right hepatic lobe, the left kidney, the subcutaneous fat of the left flank and the right paraspinous musculature (Figure 3). ROIs were placed in homogeneous regions of parenchyma or fat to avoid overlapping on any masses, blood vessels or areas of fat stranding. The ROI placement on the reduced dose series was matched exactly because the ROIs were derived from the same dataset. ROI placement on the standard dose images was matched as closely as possible to that on the reduced dose series. All measurements were performed by a single observer (medical physicist with 10 yrs CT experience, under the supervision/cross check of an abdominal imager, 17 yrs experience).

Evaluation of subjective image quality was performed by two independent experienced fellowship trained abdominal radiologists (18, 8 yrs of experience respectively, different radiologists than the one supervising noise measurements) blinded to the reduced dose (RD) series reconstruction type (i.e., RD-FBP, RD-ASIR, and RD-PICCS). For the images of each human subject, the review order of the three dose reduced image series presented to the two readers was randomized by patient, meaning that the order of series presented to the reader varied by patient. The readers were asked to read through all 50 subjects with one randomized image series before they started to read a second series on the same set of 50 patients. Image quality was graded on a five-point Likert scale from 0 to 4 (0 for non-diagnostic, 1 for severe artifact with low confidence, 2 for moderate artifact or moderate diagnostic confidence, 3 for mild artifact or high confidence, and 4 for well seen without artifacts and high confidence of detecting a lesion > 5mm) as reported previously by Flicek et al (33). The standard dose series was also reviewed and was used as the reference standard. To improve separation, 0.5 interval scores were allowed. Images were assessed in the transverse (axial) plane at the level of the main portal vein and the sacroiliac joints, and in the coronal plane at the level of the kidneys and portal vein bifurcation on each series in

soft tissue windows (width=400 HU, level=50 HU) (Figure 2, 4). Although assessments were made at these specific levels, the entire data set was available and readers could scroll through all the images at the time of their image quality assessment. This made for four image quality scores per series, times four series, times two readers, for a total of 32 subjective scores per patient. We used a cutoff at 2.5 to differentiate unacceptable from acceptable image quality.

Assessment of diagnostic accuracy was performed using focal organ-based lesion detection by the same two readers. As with the image quality assessment, the three reduced dose series (RD-FBP, RD-ASIR, RD-PICCS) were independently reviewed for focal lesions in random order. The readers were blinded to the reconstruction type and patient information was removed from the images. A minimum washout period of 3 days was mandatory between reviewing series on the same patient, but in likely all cases, at least a week passed between intra-patient assessments. After review of the three randomized reduced dose series for each patient, the standard-dose FBP images were reviewed for focal lesions to serve as the reference standard. Focal lesions for the purpose of this study were defined as high or low attenuation non-calcified parenchymal lesions measuring > 3mm in the liver, pancreas or kidneys. A maximum of 7 lesions per organ were counted. Focal calcifications were not included in this analysis. Individual and pooled lesion detection on the reduced dose series were compared to the standard dose FBP images (SD-FBP reference standard) and with the other reduced dose reconstructions.

Statistical Analysis

Summary statistics (minimum, maximum, quartiles, mean, standard deviation) were used to describe continuous variables; percentages and 95% adjusted Wald confidence intervals (35) were used for categorical variables. Image quality was considered as a numerical variable. Linear mixed effects models (36) were used to assess differences in continuous responses between reconstruction methods. These models take into account the correlation arising from using multiple reconstructions of multiple structures or tissues within the same subject. The models were fitted by maximum likelihood and an independence working correlation structure was used. Noise (HU SD), reconstruction method, tissue (fat, kidney, liver, muscle), and their interactions were included as deterministic effects, while subject was considered as a random or stochastic effect. For image quality, a sequential model-building approach was used. First, reconstruction method was the sole fixed predictor in the baseline model. Then, inclusion of attribute (location, plane of reconstruction) and the reconstruction by attribute interaction were tested in turn, via a likelihood ratio F-test; a subject-dependent intercept term was the random effect in all models. Separate models were fitted to each of the two readers. For both responses, the models were parameterized with RD-PICCS as the reference value, so that p-values are for comparisons of RD-PICCS against other reconstruction methods. For tissue and attribute, the first value in alphabetical order is the reference value.

For lesion detection, percentage of lesion detection relative to SD-FBP was computed by first combining the lesions detected in liver, pancreas, and each of the two kidneys; 95% adjusted Wald confidence intervals for the proportion were obtained (35). This was done

separately for each reader, as well as for their pooled data. Disjointness (non-overlap) of two 95% confidence intervals was taken to represent statistically significant differences at the 5% level. Also, a Wilcoxon sign (paired) test was used to compare the number of pooled lesions detected between each of the low-dose reconstructions and SD-FBP.

$P < 0.05$ (two-sided) was the criterion for statistical significance. Residual and exploratory plots were obtained to assess possible violations in test assumptions. All statistical analysis and graphics were obtained in R 2.12.1 (37).

Results

The radiation dose metrics for the reduced dose series compared to the standard series as well as the effective diameter for each patient are summarized in Table 2. The mean DLP, $CTDI_{vol}$, and SSDE for the RD series was 140.3 mGy*cm (median 79.4, range 15.9-526.6), 3.7 mGy (median 1.8, range 0.4-26.4), and 4.15 mGy (median 2.31 range 0.59-24.3) compared to 493.7 mGy*cm (median 345.8, range 57-1400.5), 12.9 mGy (median 7.9 mGy, range 1.43-79.8) and 14.6 mGy (median 10.1, range 2.1-73.4) for the SD series respectively (effective diameter was the same for the two groups). The mean effective diameter of the cohort was 30.1 cm (median 30, range 24.6-38.0). If mean SSDE is used as a conservative comparison metric, the overall dose reduction is roughly 72% (1-(4.1/14.6)) ($p<0.001$). When the studies are divided into unenhanced (urolithiasis and CT colonography protocols) compared with contrast-enhanced indications (cancer surveillance, follow up focal liver lesions, etc), greater dose reduction can be seen on the non-contrast scans where high contrast tasks are being performed (Table 3). For example, the mean SSDE for the RD non contrast series was 1.6 ± 0.7 mGy (median 1.8, range 0.6-2.9), compared to 8.6 ± 4.2 mGy (median 9.4, range 2.1-18.3) for the SD series (roughly 81% mean and median dose reduction). More modest mean and median SSDE reductions of roughly 68% and 71% were seen in the contrast enhanced group (which also included slightly larger patients, mean and median BMI 29.6 and 28.6). The highest dose levels were seen in large patients in the IV contrast group (BMI up to 43.4).

Mean image noise (averaged across all 4 sites) was lowest on the RD-PICCS series measuring 13.9±3.4 HU, compared to 57.2±23.1 on the RD-FBP series and 44.1±13.9 on the RD-ASIR series (75% noise reduction compared to RD-FBP), $p<0.001$. Noise was also reduced compared to the SD-FBP series which measured 28.6±9.6 (Table 4). Noise differences between the RD-PICCS and the other series were even more pronounced on the unenhanced CT images (Table 4) with fairly constant noise reduction across technique seen with PICCS. In addition, noise reduction did not lead to any change in the measured ROI HU attenuation when compared to the RD-FBP series (Table 5). For all ROIs, HU values measured on the RD-PICCS and RD-ASIR series were less than 5 HU different from the RD FBP series. This falls within the acceptable range (± 5HU) for the ACR requirement on CT number accuracy for quality assurance purposes.

Mean subjective image quality scores are summarized in Table 6 by reconstruction technique, plane of reformat, and location. Based on the 0-4 scale, the RD-PICCS series had improved image quality over the RD-FBP and RD-ASIR series, with mean pooled scores of

2.8±0.5 compared to 1.7 ±0.7 and 1.9±0.8 respectively ($p<0.001$). The overall mean difference between the RD-PICCS and the SD-FBP was 0.7 (SD-FBP mean score 3.5±0.5, $p<0.001$). Image quality scores were lower for the unenhanced CT images compared to the enhanced CT images (Table 6). The mean overall RD-PICCS score was 3.1±0.34, improved compared to RD-FBP (2.0±0.6) and RD-ASIR (2.3±0.6) ($p<0.001$) in the contrast enhanced cohort. The RD-PICCS series also compared favorably to the SD-FBP mean score of 3.7 ±0.3 in this cohort. Using a threshold of 2.5 for acceptable image quality, the PICCS algorithm is able to render most series acceptable compared to RD-FBP and RD-ASIR, particularly in the contrast enhanced cohort, despite marked dose savings. There were no differences between the two readers in terms of the trend in scoring across the reconstruction techniques (i.e., both readers ranked the reconstructions in the same order with similar offset in scores across techniques).

Table 7 shows the pooled focal lesion detection in the contrast enhanced, unenhanced and combined cohorts. Overall, 184 focal lesions (81%, 95% CI: 75-85%) were detected on the RD-PICCS series compared to the SD-FBP reference standard (228 lesions). This is more than that detected on the RD-FBP (153 lesions, 67%, 95% CI: 61-73%) and the RD-ASIR (149 lesions, 65%, 95% CI: 59-71%) series. Overall, fewer focal lesions were detected on the unenhanced CTs than the enhanced CTs (37 vs 191 on the SD-FBP reference standard), as expected. In the contrast enhanced cohort, where lesion detection is often the goal of the study, 83% of lesions were detected on the RD-PICCS series (158/191, 95% CI: 77-87%), compared to 72% (137/191, 95% CI: 65-78%) and 73% (139/191, 95% CI: 66-79%) on RD-FBP and RD-ASIR series respectively. The overall detection rate does remain significantly lower than on the SD-FBP series ($p<0.001$). Although the number of focal lesions detected differed slightly between readers (Table 8, contrast enhanced cohort by reader), there was no difference in the relative performance for each dose and reconstruction type.

Discussion

With the increasing attention to the theoretical risks of the radiation exposure related to CT, new dose reduction techniques have continued to emerge and have contributed to improving patient care with increased radiation safety. Among these new techniques, one of the most promising in recent years has been iterative reconstruction algorithms. Relatively modest dose reductions (average 25-40%) have been achieved with adaptive statistical iterative reconstruction (ASiR, GE Healthcare) and other vendor specific iterative reconstruction methods, including iterative reconstruction in image space (IRIS, SAPHIRE, Siemens Healthcare, iDose (Philips Healthcare) and adaptive iterative dose reduction (AIDR, Toshiba) (17, 24, 33, 38-41). Model-based iterative reconstruction has the potential for more dramatic dose savings (21, 22). However, these savings may come at a cost, particularly in the form of a relatively prolonged reconstruction time.

We previously retrospectively evaluated an alternative, vendor neutral noise reduction algorithm (PICCS) and found the potential to reduce noise 3-fold with preservation of spatial resolution and ROI HU attenuation, as well as improved image quality compared with standard FBP CT colonography images (28). Given the potential for dose reduction

suggested by that retrospective work, we are now evaluating this algorithm in a prospective fashion with a goal of validating its use in more substantially dose reduced abdominal CT.

Although not widely discussed, one of the major ongoing challenges with dose reduction is balancing the decrease in radiation with maintenance of diagnostic performance. It is important to realize that the commonly used substitute of image quality does not necessarily correlate with diagnostic performance (21), as illustrated by our results as well. In other words, a more pleasing image to the radiologist as determined by subjective image quality or objective image noise may not necessarily translate into improved diagnostic ability. Therefore, one of the primary endpoints in this study was the assessment of focal lesion detection in low contrast settings (i.e., detection of parenchymal masses in oncologic patients) to directly determine diagnostic performance. As opposed to the artificial setting of introducing noise to standard dose series in order to model dose reduction, an actual reduced dose series was undertaken in this study and directly compared against the current standard. A major advantage of the study design is that the matching reduced dose series was obtained immediately following the standard dose series, which optimizes the comparison of lesion depiction. This preliminary report is meant to assess whether our initial goal of 70-90% dose reduction was reasonable going forward with this clinical trial.

Our study results clearly demonstrate that PICCS is able to substantially decrease noise, improve image quality, and improve diagnostic performance in reduced dose series compared with the reduced dose FBP and 40% ASIR, but at the cost of decreased lesion detection compared to standard dose images. This is in the setting of fairly aggressive dose reduction where the mean SSDE decreased by over 70% where either FBP alone or ASIR was not applicable. The image quality scores and focal lesion detection rates obtained with PICCS are comparable to preliminary reports in the literature using MBIR (21). As reported by Pickhardt et al, the mean subjective image quality score with MBIR of 3.0±0.5 with similar radiation dose reduction is not significantly different from that of PICCS. Both PICCS and MBIR demonstrated similar detection rates for focal lesions (21), although both showed detection rates lower than the standard FBP series.

However, it is important to recognize that when compared with the standard dose FBP reference standard (which represents current standard-of-care), focal lesion detection was affected by the reduction in dose at these levels where lesions were missed. Thus, it appears that a trade-off exists with current dose reduction technology where markedly decreasing dose leads to poorer lesion detection compared to standard dose protocols in low contrast settings (i.e., lesion detection in parenchymal organs). This decrease in lesion detection is seen in spite of the fact that PICCS actually reduces noise compared to the SD FBP series. The explanation for this phenomenon may be related to a smoothing of the interface between the low contrast lesion and the adjacent parenchyma on the background of decreased overall contrast, as a price paid for the noise reduction. This in turn leads to a lack of recognition of a focal lesion and instead is interpreted as a geographic area of mottled attenuation within normal variation by a reader.

This result points to the need to potentially tailor the amount of dose reduction to the indication for the study given the limitations of current dose reduction technology. More

aggressive dose reduction can be undertaken when the focus is in high contrast imaging tasks such as in assessment of renal calculi, active Crohn's disease, abdominal vessels (CT angiography) or colorectal cancer screening with CT colonography, whereas less dose reduction may be attempted in low contrast setting such as focal parenchymal lesion detection in oncologic surveillance (Figure 5). Recently, Baker et al reported that detection of small or low contrast lesions is more heavily impacted by reductions in dose than detection of larger lesions or those with greater contrast compared to background (42). As we continue to accrue patients in this trial, we hope to be able to compare discrete cohorts according to specific clinical indication and technique (ie, CT colonography, flank pain CT, versus contrast enhanced CT for oncology follow up etc) to evaluate these dose reduction goals based on diagnostic performance for these individualized tasks. In addition to indication, the individual patient characteristics (age, BMI, disease status, possibly cumulative dose) need to be considered in the dose prescription.

With regard to image quality, many of these iterative reconstruction algorithms have a smoothing effect on the images, which to some readers is unappealing and which can be difficult to capture with image quality scores or noise measurements. Although image quality scores are favorable with PICCS, this smoothing effect is present and may not be acceptable to some readers (Figs 2,4,5). This can be a challenge in implementation given the varying preferences of radiologists in a single division, department or practice.

There is no significant change in quantitative assessments such as ROI HU attenuation seen with the PICCS and ASIR algorithms. All measurements were within 5 HU, which is the acceptable range for CT number quality assurance.

PICCS has several specific strengths. The PICCS reconstruction is vendor neutral and can be performed using DICOM image data in a matter of minutes. In addition, as above, all CT number measurements on RD-PICCS were within 5 HU of those measured on RDFBP.

There are a number of limitations to this study. These data represent an early interim analysis of an ongoing prospective clinical trial with a target enrollment of 500 subjects. Therefore, this remains a relatively small sample size and a somewhat heterogeneous population given the differences in technique. Lesion specific matching was not performed between readers and with the SD FBP reference standard, and we have not yet investigated the possibility of false positive findings on the reduced dose series. Lesion characterization and size measurement were not attempted in this initial analysis. Although we did not specifically address preservation of spatial resolution at low doses using PICCS in this study, we have looked at it in the past using phantoms (28). On contrast enhanced studies, we have only used the portal venous phase and have not yet evaluated arterial or delayed phases of multiphasic exams. This will hopefully be a part of future work during the course of this trial. The patients were not re-injected with contrast, therefore, there may have been slight differences in the phase of contrast between the standard and low dose images. Images were obtained in the same breath hold to minimize this. Although there was a washout period employed before readers rereviewed the same patient images, there is still the potential for memory effects.

In summary, PICCS shows potential for substantially decreasing radiation dose at abdominal CT. The amount of dose reduction achieved must be weighed against the clinical indication of the exam, and requires additional study. However, any additional study in dose reduction should include a metric for diagnostic performance in addition to assessments of image noise and image quality.

Acknowledgments

This work was partially supported by NIH grant funding R01CA169331.

Appendix 1

Abdominal MDCT "standard-dose" protocols utilized in the prospective trial*

Protocol:	IV Contrast	Urolithiasis	Supine CTC
Scanner	GE HD750	GE HD 750	GE HD 750
Scan Type	Helical	Helical	Helical
Rotation Time (sec)	0.5	0.8	0.5
Beam Collimation (mm)	40	40	40
Detector Rows	64	64	64
Pitch	0.516	0.516	0.984
Speed (mm/rot)	20.64	20.64	39.36
Detector Configuration	64 × 0.625	64 × 0.625	64 × 0.625
Slice Thickness for NI (mm)	1.25	1.25	1.25
Scan FOV	Large Body	Large Body	Large Body
kV_p	120	120	120
Smart mA Range	60-660	40-660	30-300
Noise Index	24	28	50
Reconstructions (FBP):			
DFOV	36-50	36-50	36-50
Recon Type	Standard	Standard	Standard
Window W/L	400/50	400/50	400/50
Recon Option	Plus	Plus	Plus
Slice Thickness (mm)	2.5	2.5	2.5
Interval (mm)	1.5	1.5	1.5

* The specific protocol for the accompanying low-dose series was derived by adjusting the noise index (NI)/slice thickness pairing (and mA range) to allow for a targeted 70-90% dose reduction (by DLP) relative to the "standard-dose" series.

References

1. Brenner DJ, Hall EJ. Computed tomography--an increasing source of radiation exposure. N Engl J Med. 2007; 357(22):2277–84. [PubMed: 18046031]
2. Mahesh M. NCRP Report Number 160: its significance to medical imaging. J Am Coll Radiol. 2009; 6(12):890–2. [PubMed: 19945048]

3. Ionizing radiation exposure of the population of the United States. Bethesda, MD: 1987. Measurements NCoRPa.
4. Pearce MS, Salotti JA, Little MP, et al. Radiation exposure from CT scans in childhood and subsequent risk of leukaemia and brain tumours: a retrospective cohort study. Lancet. 2012; 380(9840):499–505. [PubMed: 22681860]
5. McCollough CH, Primak AN, Braun N, Kofler J, Yu L, Christner J. Strategies for reducing radiation dose in CT. Radiol Clin North Am. 2009; 47(1):27–40. [PubMed: 19195532]
6. Mulkens TH, Bellinck P, Baeyaert M, et al. Use of an automatic exposure control mechanism for dose optimization in multi-detector row CT examinations: clinical evaluation. Radiology. 2005; 237(1):213–23. [PubMed: 16126917]
7. McCollough CH, Bruesewitz MR, Kofler JM Jr. CT dose reduction and dose management tools: overview of available options. Radiographics. 2006; 26(2):503–12. [PubMed: 16549613]
8. Graser A, Wintersperger BJ, Suess C, Reiser MF, Becker CR. Dose reduction and image quality in MDCT colonography using tube current modulation. AJR Am J Roentgenol. 2006; 187(3):695–701. [PubMed: 16928932]
9. Greess H, Wolf H, Baum U, et al. Dose reduction in computed tomography by attenuation-based on-line modulation of tube current: evaluation of six anatomical regions. Eur Radiol. 2000; 10(2):391–4. [PubMed: 10663775]
10. McCollough CH. Automatic exposure control in CT: are we done yet? Radiology. 2005; 237(3): 755–6. [PubMed: 16304094]
11. Gies M, Kalender WA, Wolf H, Suess C. Dose reduction in CT by anatomically adapted tube current modulation. I. Simulation studies. Med Phys. 1999; 26(11):2235–47. [PubMed: 10587204]
12. Kalender WA, Wolf H, Suess C. Dose reduction in CT by anatomically adapted tube current modulation. II. Phantom measurements. Med Phys. 1999; 26(11):2248–53. [PubMed: 10587205]
13. Haaga JR, Miraldi F, MacIntyre W, LiPuma JP, Bryan PJ, Wiesen E. The effect of mAs variation upon computed tomography image quality as evaluated by in vivo and in vitro studies. Radiology. 1981; 138(2):449–54. [PubMed: 7455129]
14. Goetti R, Winklehner A, Gordic S, et al. Automated attenuation-based kilovoltage selection: preliminary observations in patients after endovascular aneurysm repair of the abdominal aorta. AJR Am J Roentgenol. 2012; 199(3):W380–5. [PubMed: 22915430]
15. Supanich M, Tao Y, Nett B, et al. Radiation dose reduction in time-resolved CT angiography using highly constrained back projection reconstruction. Phys Med Biol. 2009; 54(14):4575–93. [PubMed: 19567941]
16. Marin D, Nelson RC, Schindera ST, et al. Low-tube-voltage, high-tube-current multidetector abdominal CT: improved image quality and decreased radiation dose with adaptive statistical iterative reconstruction algorithm--initial clinical experience. Radiology. 2010; 254(1):145–53. [PubMed: 20032149]
17. Prakash P, Kalra MK, Kambadakone AK, et al. Reducing abdominal CT radiation dose with adaptive statistical iterative reconstruction technique. Invest Radiol. 2010; 45(4):202–10. [PubMed: 20177389]
18. Silva AC, Lawder HJ, Hara A, Kujak J, Pavlicek W. Innovations in CT dose reduction strategy: application of the adaptive statistical iterative reconstruction algorithm. AJR Am J Roentgenol. 2010; 194(1):191–9. [PubMed: 20028923]
19. Thibault JB, Sauer KD, Bouman CA, Hsieh J. A three-dimensional statistical approach to improved image quality for multislice helical CT. Med Phys. 2007; 34(11):4526–44. [PubMed: 18072519]
20. Chen GH, Tang J, Leng S. Prior image constrained compressed sensing (PICCS): a method to accurately reconstruct dynamic CT images from highly undersampled projection data sets. Med Phys. 2008; 35(2):660–3. [PubMed: 18383687]
21. Pickhardt PJ, Lubner MG, Kim DH, et al. Abdominal CT with model-based iterative reconstruction (MBIR): initial results of a prospective trial comparing ultralow-dose with standard-dose imaging. AJR Am J Roentgenol. 2012; 199(6):1266–74. [PubMed: 23169718]

22. Chang W, Lee JM, Lee K, et al. Assessment of a Model-Based, Iterative Reconstruction Algorithm (MBIR) Regarding Image Quality and Dose Reduction in Liver Computed Tomography. Invest Radiol. 2013
23. Hara AK, Paden RG, Silva AC, Kujak JL, Lawder HJ, Pavlicek W. Iterative reconstruction technique for reducing body radiation dose at CT: feasibility study. AJR Am J Roentgenol. 2009; 193(3):764–71. [PubMed: 19696291]
24. Sagara Y, Hara AK, Pavlicek W, Silva AC, Paden RG, Wu Q. Abdominal CT: comparison of low-dose CT with adaptive statistical iterative reconstruction and routine-dose CT with filtered back projection in 53 patients. AJR Am J Roentgenol. 2010; 195(3):713–9. [PubMed: 20729451]
25. Kambadakone AR, Chaudhary NA, Desai GS, Nguyen DD, Kulkarni NM, Sahani DV. Low-dose MDCT and CT enterography of patients with Crohn disease: feasibility of adaptive statistical iterative reconstruction. AJR Am J Roentgenol. 2011; 196(6):W743–52. [PubMed: 21606263]
26. Mitsumori LM, Shuman WP, Busey JM, Kolokythas O, Koprowicz KM. Adaptive statistical iterative reconstruction versus filtered back projection in the same patient: 64 channel liver CT image quality and patient radiation dose. Eur Radiol. 2012; 22(1):138–43. [PubMed: 21688003]
27. McCollough CH, Chen GH, Kalender W, et al. Achieving routine submillisievert CT scanning: report from the summit on management of radiation dose in CT. Radiology. 2012; 264(2):567–80. [PubMed: 22692035]
28. Lubner MG, Pickhardt PJ, Tang J, Chen GH. Reduced image noise at low-dose multidetector CT of the abdomen with prior image constrained compressed sensing algorithm. Radiology. 2011; 260(1):248–56. [PubMed: 21436086]
29. McCollough, C.; Cody, D.; Edyvean, S., et al. American Association of Physicists in Medicine. AAPM; College Park, MD: 2008. The measurement, reporting and mangement of radiation dose in CT.
30. Deak PD, Smal Y, Kalender WA. Multisection CT protocols: sex- and age-specific conversion factors used to determine effective dose from dose-length product. Radiology. 2010; 257(1):158–66. [PubMed: 20851940]
31. Boone, JMSK.; Cody, DD.; McCullough, CH.; McNitt-Gray, MF.; Toth, TL. American Association of Physicists in Medicine. American Association of Physicists in Medicine; College Park MD: 2011. Size-Specific Dose Estimates (SSDE) in Pediatric and Adult Body CT Examinations.
32. Bankier AA, Kressel HY. Through the Looking Glass revisited: the need for more meaning and less drama in the reporting of dose and dose reduction in CT. Radiology. 2012; 265(1):4–8. [PubMed: 22993216]
33. Flicek KT, Hara AK, Silva AC, Wu Q, Peter MB, Johnson CD. Reducing the radiation dose for CT colonography using adaptive statistical iterative reconstruction: A pilot study. AJR Am J Roentgenol. 2010; 195(1):126–31. [PubMed: 20566805]
34. Tang JT-LP, Chen G-H. Proc. SPIE 7961, Medical Imaging. Physics of Medical Imaging. 2011
35. Agresti ACB. Approximate is Better than “Exact” for Interval Estimation of Binomial Proportions. The American Statistician. 1998; 52(2):119–26.
36. Pinheiro, JCBD. Mixed-Effects Models in S and S-PLUS. Springer; New York: 2000.
37. Team RDC. R: A language and environment for statistical computing. Computing RFfS. Vienna, Austria: 2009.
38. Singh S, Kalra MK, Hsieh J, et al. Abdominal CT: comparison of adaptive statistical iterative and filtered back projection reconstruction techniques. Radiology. 2010; 257(2):373–83. [PubMed: 20829535]
39. Noel PB, Fingerle AA, Renger B, Munzel D, Rummeny EJ, Dobritz M. Initial performance characterization of a clinical noise-suppressing reconstruction algorithm for MDCT. AJR Am J Roentgenol. 2011; 197(6):1404–9. [PubMed: 22109296]
40. Lee SJ, Park SH, Kim AY, et al. A prospective comparison of standard-dose CT enterography and 50% reduced-dose CT enterography with and without noise reduction for evaluating Crohn disease. AJR Am J Roentgenol. 2011; 197(1):50–7. [PubMed: 21701010]

41. Gervaise A, Osemont B, Lecocq S, et al. CT image quality improvement using Adaptive Iterative Dose Reduction with wide-volume acquisition on 320-detector CT. Eur Radiol. 2012; 22(2):295–301. [PubMed: 21927791]

42. Baker ME, Dong F, Primak A, et al. Contrast-to-noise ratio and low-contrast object resolution on full- and low-dose MDCT: SAFIRE versus filtered back projection in a low-contrast object phantom and in the liver. AJR Am J Roentgenol. 2012; 199(1):8–18. [PubMed: 22733888]

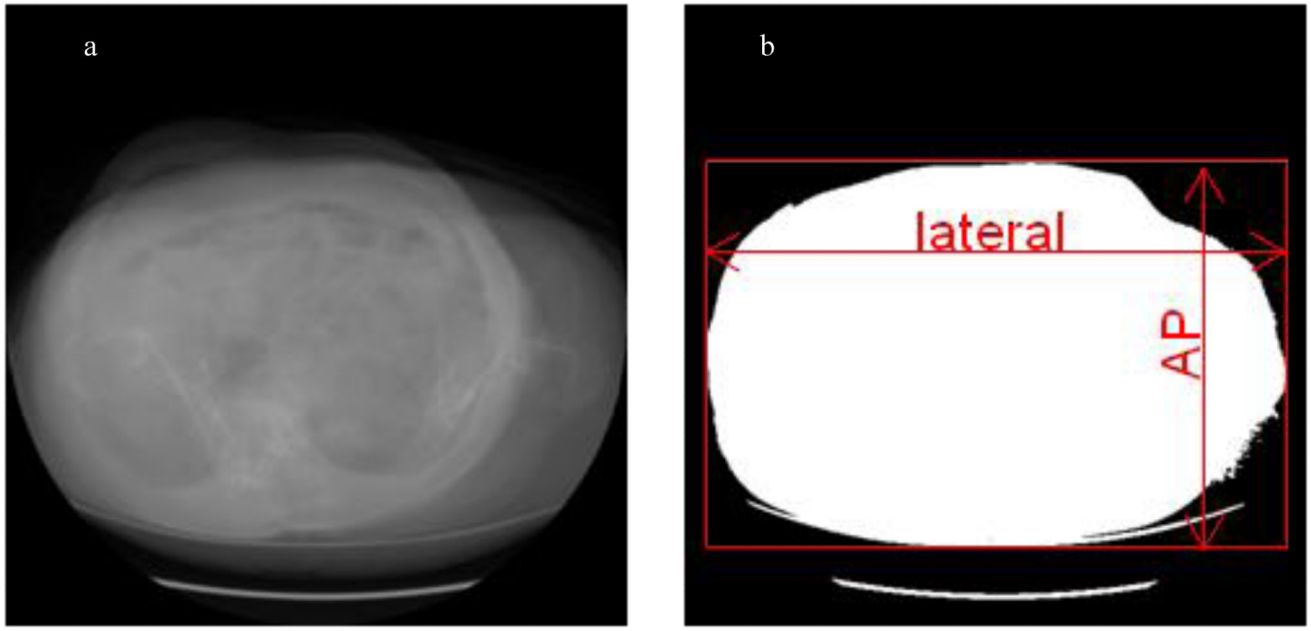

Figure 1.

Determination of effective diameter. Images demonstrate averaged CT image volume along z-direction with display windows: (a) W/L=2000/0 HU (b) W/L=0/−400 HU. The average AP and lateral dimensions were measured on (b) and used in the calculation of effective diameter.

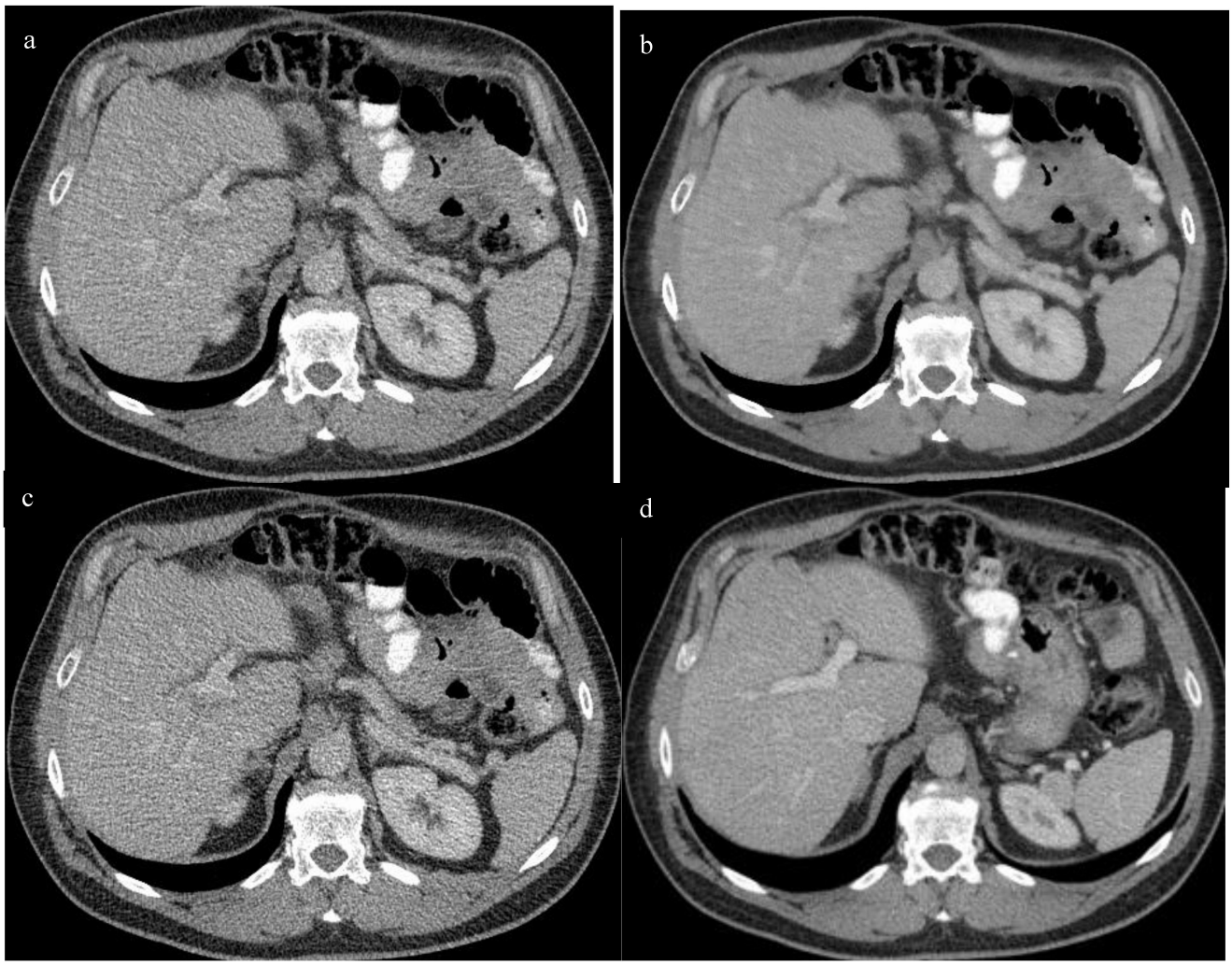

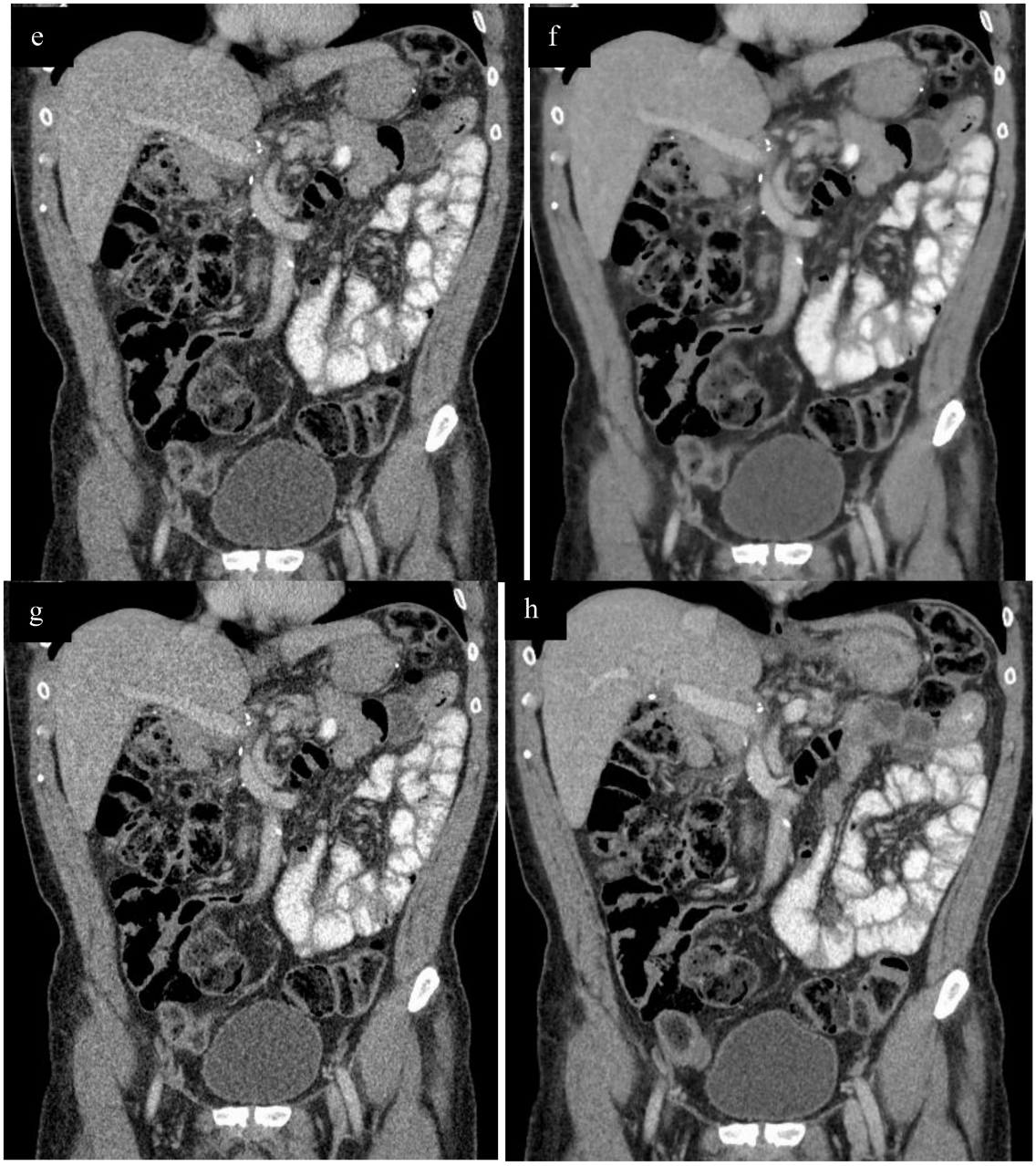

Figure 2.

Axial contrast enhanced CT in portal venous phase at the level of the main portal vein, with reduced dose series reconstructed with ASIR (a), PICCS (b), FBP (c) and standard dose FBP (d). Corresponding coronal images at the level of the portal vein are also shown (e, RD ASIR; f, RD PICCS; g, RD FBP; h, SD FBP). Images were obtained in a 54 yr old male with a BMI of 31.8 and an effective diameter of 30.4. SSDE for the reduced dose series was 5.3 mGy, compared to 13.4 mGy for the standard dose series, with an approximate dose reduction of 60% in this obese patient.

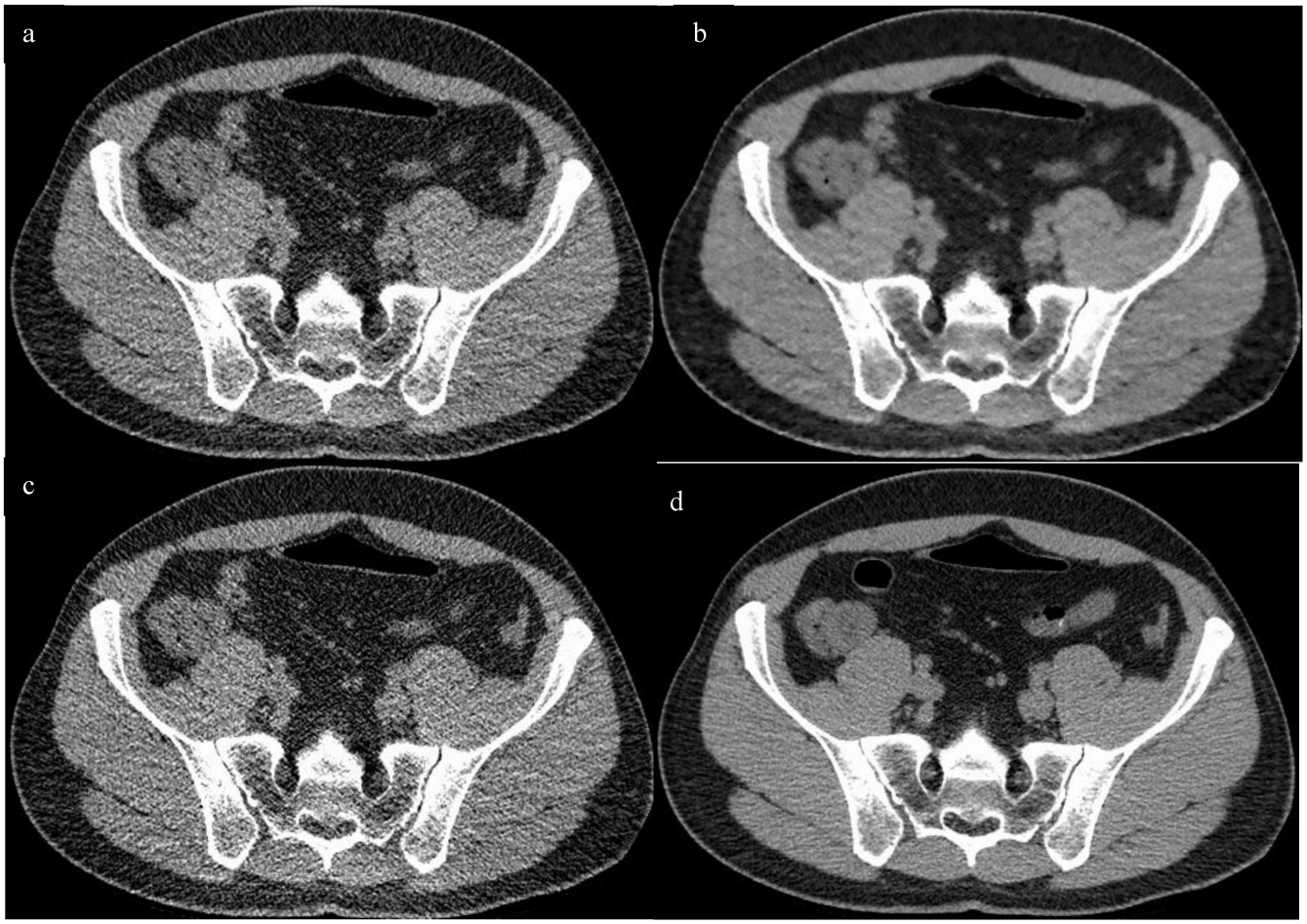

Figure 3.

Axial CE CT images with 250 mm^2 regions of interest (ROI, red circle) on the liver (a), left kidney (b), right paraspinous muscle (c) and left flank subcutaneous fat (d). These were replicated exactly on the reduced dose series for a given patient and approximated as closely as possible on the standard dose series and across patients. These images were the reduced dose series reconstructed with filtered back projection (RD FBP) in a 63 yr old female pt with BMI of 38.8 and effective diameter of 35.5. SSDE for the reduced dose series was 8.6 mGy, compared to the standard dose series dose of 21.7 mGy, with a dose reduction of approximately 60%.

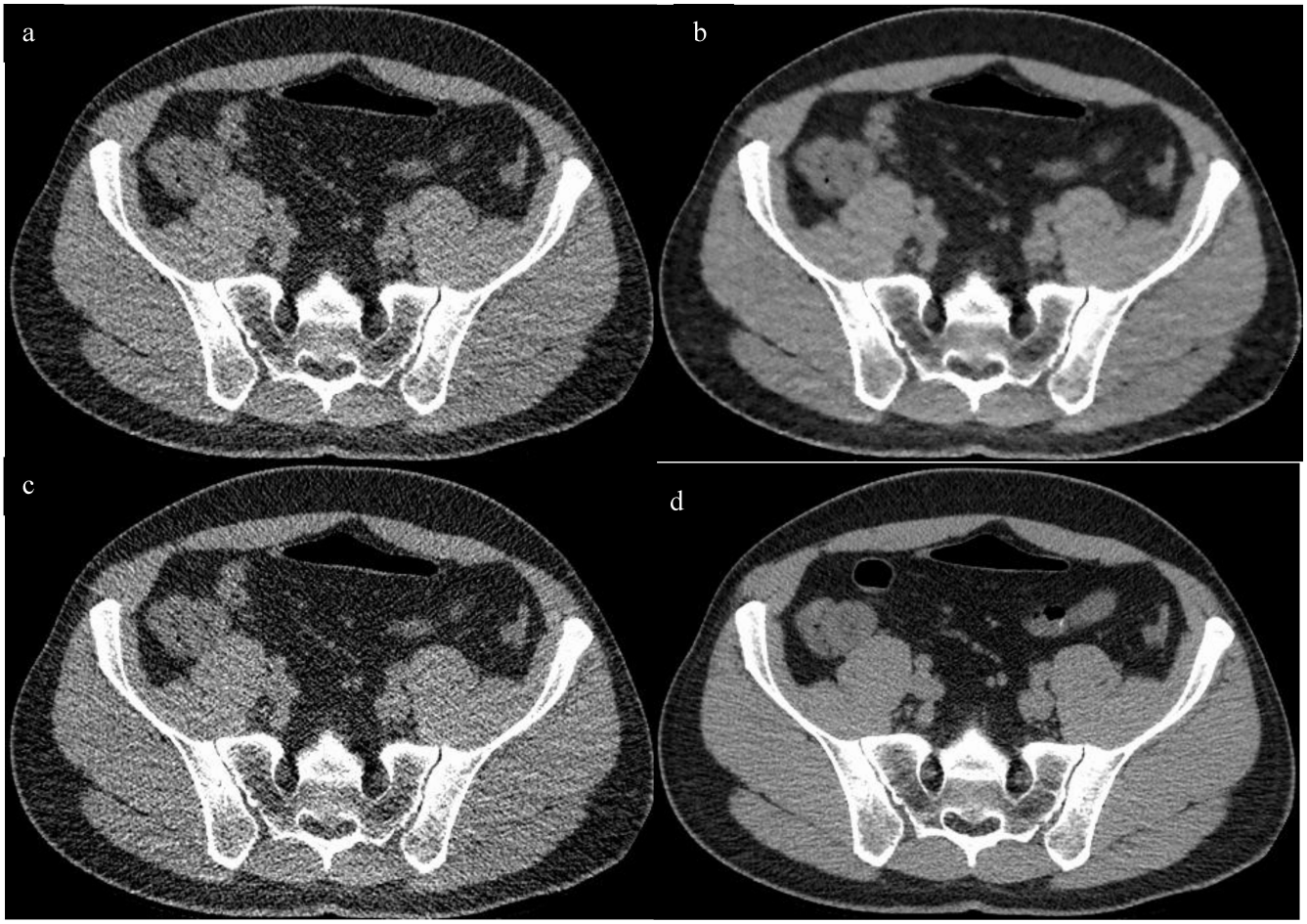

Figure 4.

Non contrast images from a 41 year old male with a BMI of 28.8 and effective diameter of 29.6 cm undergoing a flank pain protocol to evaluate for urolithiasis. Transverse CT images were obtained at the level of the sacroiliac joint, with the reduced dose reconstructed with ASIR (a), PICCS (b), FBP (c) compared to the standard dose FBP image (d). Coronal images obtained at the level of the kidneys with corresponding reconstructions (RD ASIR e, RD PICCS f, RD FBP g, SD FBP h). Note the small calculus in the interpolar region of the right kidney (arrows, e-h). Images were also evaluated in the transverse and coronal planes at the level of the main portal vein as depicted in figure 2. The SSDE of the reduced dose series was 1.8 mGy, compared to 9.7 for the standard dose, a dose reduction of approximately 81%.

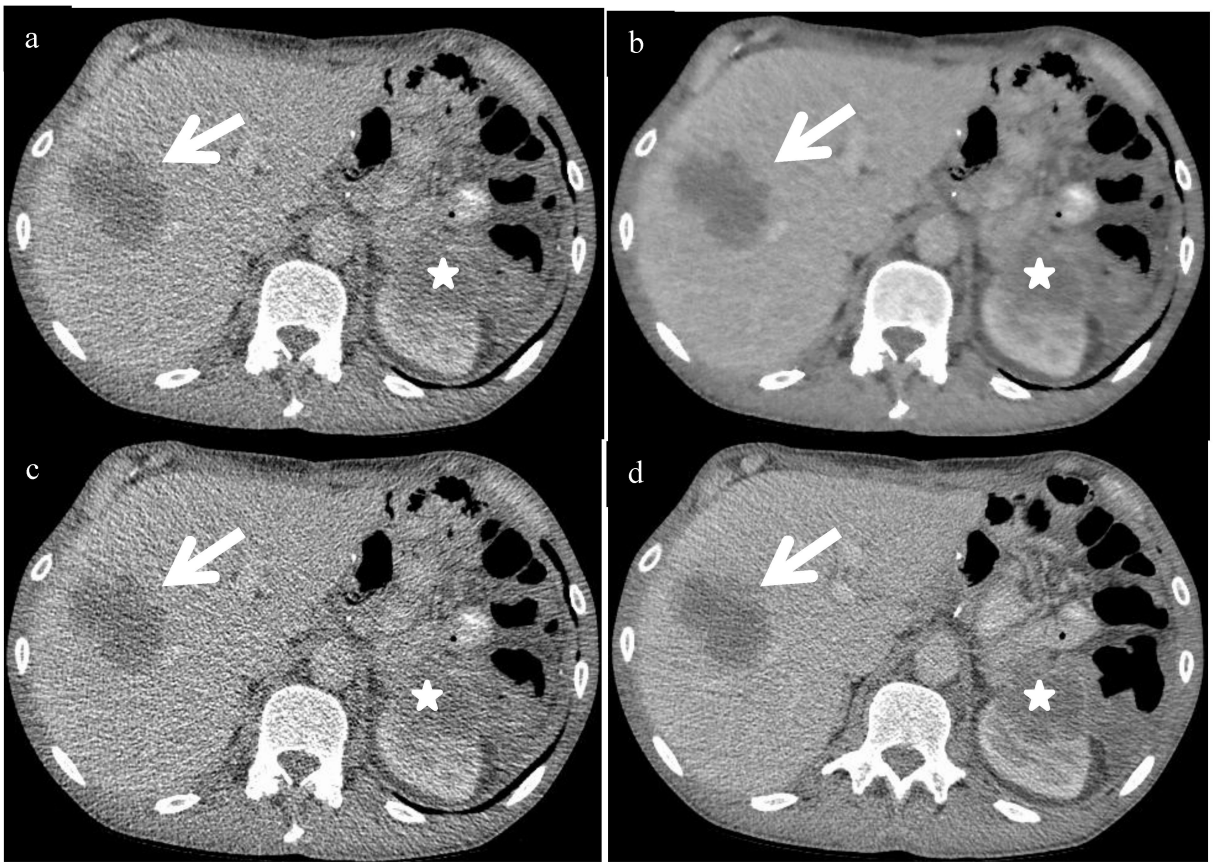

Figure 5.

Contrast enhanced axial CT images of the liver in a 52 yr old male patient s/p distal pancreatectomy and splenectomy for pancreatic adenocarcinoma with a BMI of 22 and an effective diameter of 24.9. Reduced dose images reconstructed with ASIR (a), PICCS (b), FBP (c) demonstrate an ill-defined low attenuation liver lesion which is identifiable on all series (arrows) and redemonstrated on the standard dose FBP image (d). This lesion measures roughly 50 HU compared to the background liver (95 HU) and is large enough to be well seen, but as lesions decrease in size and become closer in attenuation to background, they become more difficult to see. Note the low attenuation lesion at the upper pole of the left kidney along the post-operative bed (*) that starts to blend in to the adjacent low attenuation bowel on the reduced dose series. Both lesions were metastatic pancreas cancer. The SSDE in the reduced dose series was 2.1 mGy, compared to the standard dose series of 7.0 mGy, for a dose reduction of 70%.

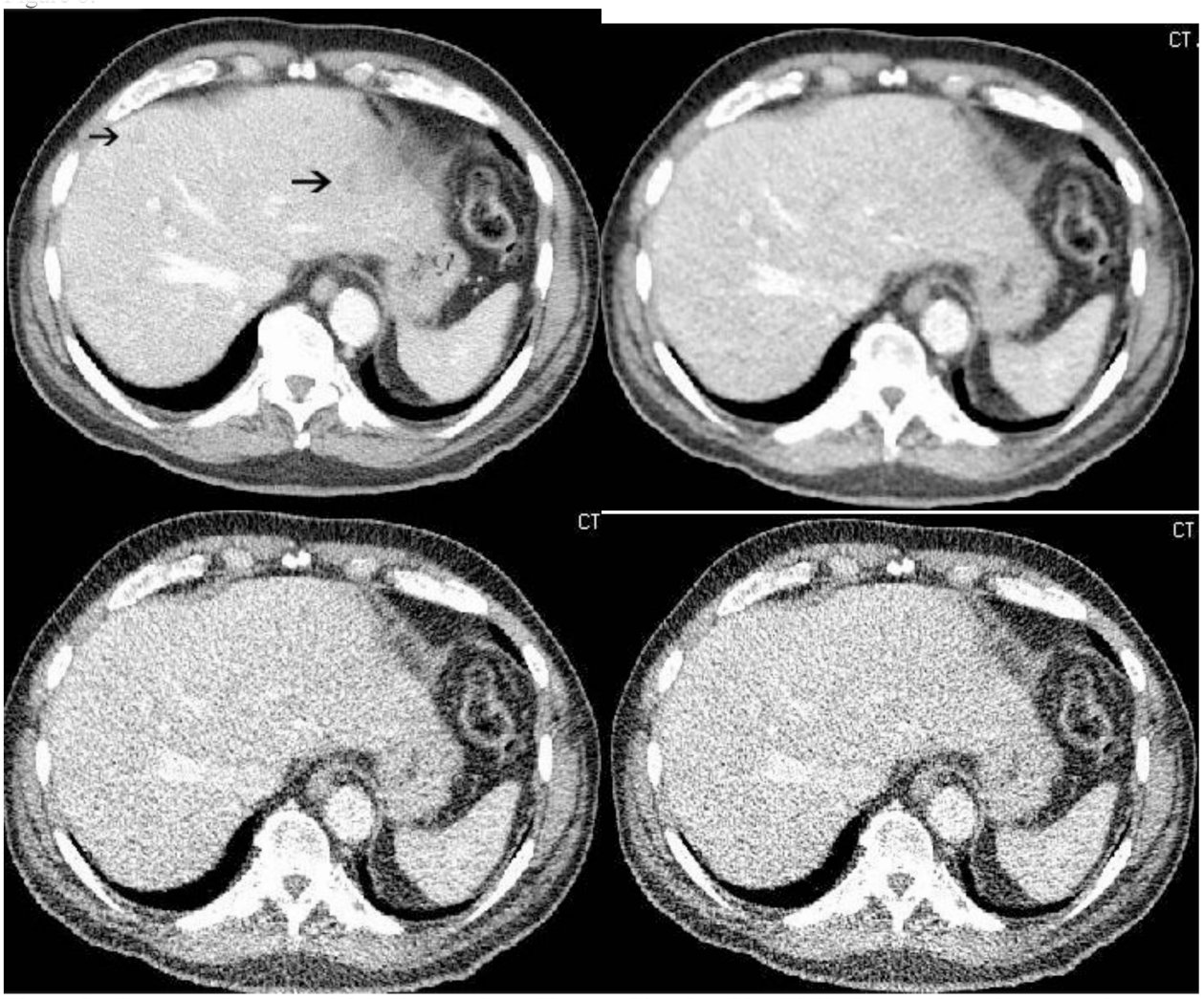

Figure 6.

Contrast enhanced axial CT images in an 82 year old male with a BMI of 28 and hepatic metastatic neuroendocrine tumor. SD-FBP image (a) demonstrates two vague low attenuation lesions (arrows) that are not well seen on the LD-PICCS (b), LD-ASIR (c) or LD-FBP (d) images. Multiple additional liver lesions (not shown here) were also not well seen on the low dose images. The SD DLP was 433, the LD DLP was 133 for a dose reduction of approximately 75%.

Table 1

Patient Characteristics

Patient number	Age	Sex	Ht (in)	Wt (lbs)	BMI	Study protocol	IV contrast admin
1	71	M	69	259	38.2	VC	N
2	42	M	73	185	24.4	VC	N
3	56	F	68	142	21.6	VC	N
4	71	F	64	177	30.4	VC	N
5	62	F	67	223	34.9	VC	N
6	50	F	67	200	31.3	VC	N
7	52	M	65	149	24.8	VC	N
8	51	F	64	140	24.0	VC	N
9	59	M	71	170	23.7	VC	N
10	55	M	67	200	31.3	VC	N
11	86	F	64	164	28.1	St	N
12	42	M	69	174	25.7	St	N
13	28	M	74	203	26.1	St	N
14	58	F	63	149	26.4	St	N
15	80	M	70	178	25.5	St	N
16	71	M	72	232	31.5	St	N
17	29	M	74	216	27.7	St	N
18	62	M	74	162	20.8	St	N
19	59	F	60	175	34.2	St	N
20	43	F	67	169	26.5	St	N
21	63	F	64	226	38.8	IV	Y
22	35	F	65	139	23.1	IV	Y
23	77	F	61	127	24.0	IV	Y
24	48	M	80	238	26.1	IV	Y
25	72	F	65	216	35.9	IV	Y
26	82	M	71	204	28.4	IV	Y
27	55	F	64	232	39.8	IV	Y
28	85	F	60	173	33.8	IV	Y
29	57	M	70	290	41.6	IV	Y
30	41	F	65	146	24.3	St	N
31	66	M	75	209	26.1	St	N
32	77	F	63	170	30.1	IV	Y
33	41	M	69	195	28.8	St	N
34	63	M	68	231	35.1	IV	Y
35	79	M	70	170	24.4	IV	Y
36	39	M	73	164	21.6	IV	Y

Patient number	Age	Sex	Ht (in)	Wt (lbs)	BMI	Study protocol	IV contrast admin
37	58	F	64	113	19.4	IV	Y
38	42	M	73	213	28.1	IV	Y
39	60	F	62	129	23.6	IV	Y
40	48	M	72	179	24.3	IV	Y
41	76	M	67	178	27.9	IV	Y
42	50	F	67	211	33.0	VC	N
43	52	F	65	182	30.3	IV	Y
44	42	M	72	239	32.4	IV	Y
45	69	M	69.5	178	25.9	IV	Y
46	54	M	67	203	31.8	IV	Y
47	52	M	70	153	22.0	IV	Y
48	57	F	65	178	29.6	IV	Y
49	70	M	70	200	28.7	IV	Y
50	63	F	64	253	43.4	IV	Y
Mean	57.7	23F, 27M	67.8	186.7	28.8		24 non, 26 IV
Median	57.5				28.0		

VC=Virtual colonoscopy; St=Renal stone/flank pain protocol, IV=routine portal venous post contrast images

Table 2
Dose metrics of standard dose compared to reduced dose images

Patient #	DLP SD	DLP RD	Eff dose SD	Eff dose RD	CTDI vol SD	CTDI vol RD	Effective Diam	SSDE SD	SSDE RD
1	519.56	132.14	7.79	1.98	10.88	2.76	37.22	10.34	2.62
2	178.77	23.43	2.68	0.35	3.63	0.48	28.82	4.65	0.61
3	56.95	15.93	0.85	0.24	1.43	0.40	25.27	2.12	0.59
4	169.15	36.51	2.54	0.55	3.68	0.79	30.83	4.38	0.94
5	287.15	60.00	4.31	0.90	5.88	1.23	33.46	6.47	1.35
6	304.16	64.62	4.56	0.97	6.20	1.32	31.21	7.38	1.57
7	88.00	19.10	1.32	0.29	2.03	0.44	27.78	2.68	0.58
8	109.74	25.89	1.65	0.39	2.47	0.59	25.86	3.53	0.84
9	111.07	23.61	1.67	0.35	2.23	0.48	27.67	2.94	0.63
10	203.01	42.40	3.05	0.64	4.09	0.85	31.71	4.66	0.97
11	435.40	59.89	6.53	0.90	10.31	1.42	29.17	13.20	1.82
12	266.81	59.81	4.00	0.90	6.67	1.50	25.66	9.54	2.15
13	346.66	64.75	5.20	0.97	8.05	1.50	27.68	10.63	1.98
14	294.36	63.73	4.42	0.96	7.31	1.58	28.71	9.36	2.02
15	332.51	62.69	4.99	0.94	7.95	1.50	29.63	9.78	1.85
16	686.53	109.93	10.30	1.65	16.60	2.66	33.03	18.26	2.93
17	471.30	73.76	7.07	1.11	9.80	1.53	30.41	12.05	1.88
18	242.67	61.71	3.64	0.93	5.97	1.52	25.76	8.54	2.17
19	535.47	85.09	8.03	1.28	12.87	2.04	30.93	15.32	2.43
20	343.32	63.56	5.15	0.95	7.50	1.39	28.83	9.60	1.78
21	1070.04	426.86	16.05	6.40	21.26	8.48	35.49	21.69	8.65
22	152.25	43.35	2.28	0.65	4.54	1.29	27.01	6.22	1.77
23	197.63	62.26	2.96	0.93	4.85	1.53	26.07	6.94	2.19
24	751.06	296.87	11.27	4.45	14.33	5.66	31.49	17.05	6.74
25	1216.92	485.10	18.25	7.28	25.71	10.25	32.65	28.28	11.28
26	433.15	112.84	6.50	1.69	14.51	3.78	31.05	17.27	4.50
27	1258.40	154.51	18.88	2.32	32.09	3.94	34.24	34.02	4.18
28	674.62	287.62	10.12	4.31	35.30	15.05	32.24	40.24	17.16
29	1453.71	481.66	21.81	7.22	79.83	26.45	38.02	73.44	24.33
30	339.89	65.23	5.10	0.98	7.72	1.48	24.69	11.43	2.19
31	464.36	73.76	6.97	1.11	10.06	1.60	28.69	12.88	2.05
32	546.19	212.68	8.19	3.19	11.69	4.55	29.22	14.96	5.82
33	350.56	65.75	5.26	0.99	7.85	1.47	29.55	9.66	1.81
34	1025.01	390.50	15.38	5.86	19.55	7.71	34.37	20.72	8.17
35	341.29	133.60	5.12	2.00	7.35	2.88	28.36	9.70	3.80
36	274.31	101.00	4.11	1.52	5.39	1.98	27.22	7.38	2.71

Patient #	DLP SD	DLP RD	Eff dose SD	Eff dose RD	CTDI vol SD	CTDI vol RD	Effective Diam	SSDE SD	SSDE RD
37	202.23	48.32	3.03	0.72	4.56	1.09	24.57	6.75	1.61
38	541.68	210.39	8.13	3.16	11.59	4.56	30.50	14.26	5.61
39	250.14	91.27	3.75	1.37	5.92	2.16	25.75	8.47	3.09
40	345.04	136.52	5.18	2.05	7.29	2.88	28.53	9.33	3.69
41	991.94	241.05	14.88	3.62	41.48	10.08	32.50	47.29	11.49
42	312.47	66.09	4.69	0.99	6.17	1.31	31.68	7.03	1.49
43	496.82	89.75	7.45	1.35	17.88	3.23	30.93	21.28	3.84
44	1233.24	149.20	18.50	2.24	34.22	4.14	34.68	34.90	4.22
45	344.56	134.37	5.17	2.02	7.10	2.77	28.98	9.09	3.55
46	543.57	212.41	8.15	3.19	10.93	4.35	30.37	13.44	5.35
47	212.55	63.62	3.19	0.95	4.70	1.41	24.92	6.96	2.09
48	724.09	289.04	10.86	4.34	15.80	6.31	32.98	17.38	6.94
49	556.30	214.24	8.34	3.21	10.67	4.18	31.79	12.16	4.77
50	1400.50	526.58	21.01	7.90	27.50	11.06	36.64	26.13	10.51
Mean	493.7	140.3	7.4	2.1	12.9	3.7	30.1	14.6	4.2
Median	345.8	79.43	5.2	1.2	7.9	1.8	30	10.1	2.3

SD=Standard dose, RD=reduced dose. DLP=Dose Length Product, Eff dose=effective dose, CTDIvoi=volume CT dose index, SSDE=Size specific Dose estimate.

Table 3

Comparison of dose by contrast administration

Contrast		BMI	DLP SD	DLP RD	Eff dose SD	Eff dose RD	CTDI vol SD	CTDIvol RD	SSDE SD	SSDE RD
Non con	Mean	27.9	310.4	59.1	4.6	0.9	7.0	1.3	8.6	1.6
	Median	26.4	308.3	63.1	4.6	0.9	7.0	1.4	9.4	1.8
IV con	Mean	29.6	663.0	215.2	9.9	3.2	18.3	5.8	20.2	6.5
	Median	28.6	544.9	182.4	8.1	2.7	13.0	4.2	16.0	4.6

BMI=Body mass index, DLP=Dose Length Product, SD=Standard dose, RD=Reduced dose, Eff dose=effective dose, $CTDI_{VOI}$=volume CT dose index, SSDE=Size Specific Dose estimate.

Table 4

Mean Image Noise by Series

	With IV Contrast (n=26)				Without IV Contrast (n=24)				Overll cohort			
Location	**RD-FBP**	**RD-ASIR**	**RD-PICCS**	**SD-FBP**	**RD-FBP**	**RD-ASIR**	**RD-PICCS**	**SD-FBP**	**RD-FBP**	**RD-ASIR**	**RD-PICCS**	**SD-FBP**
Liver	43.7	46.7	13	24.2	79.4	60.3	14.9	33.9	60.8	46.6	13.9	28.8
Kidney	44.5	34.9	15.2	27.3	73	55.9	13.9	33.7	58.2	45.0	14.6	30.4
Subq fat	37.9	29.5	11.5	21.6	69.1	53.7	14.5	30.3	52.9	41.1	13.0	25.8
Muscle	42.1	32.7	13.8	25.7	73	55.8	14.8	33.3	56.9	43.8	14.3	29.4
Overall	42.1	36.0	13.4	24.7	73.6	56.4	14.5	32.8	57.2	44.1	13.9	28.6

Note: All measurements are in Hounsfield Units (HU). Image noise refers to the SD around the mean region of interest attenuation measurement. RD=Reduced dose, FBP=Filtered back projection, ASIR=Adaptive statistical iterative reconstruction, PICCS=Prior image constrained compressed sensing, SD=Standard dose

Table 5

Mean CT Number (HU) by reconstruction technique and location

Location	RD-FBP	RD-ASIR	RD-PICCS
Liver		79±25	79±25
Kidney	97±67	97±67	97±67
Fat		−100±14	−100±14
Muscle	54±14	54±14	55±14

All numbers are expressed in Hounsfield units (HU). RD=Reduced dose, FBP=Filtered back projection, ASIR=Adaptive statistical iterative reconstruction, PICCS=Prior image constrained compressed sensing.

Table 6

Mean subjective Image Quality Scores by Dose, Reconstruction, Location and Contrast administration

	IV contrast				Non contrast				Overall cohort			
Level Transverse	**RD- FBP**	**RD-ASIR**	**RD-PICCS**	**SD-FBP**	**RD- FBP**	**RD-ASIR**	**RD-PICCS**	**SD-FBP**	**RD-FBP**	**RD-ASIR**	**RD-PICCS**	**SD-FBP**
Main portal vein	1.9	2.2	3	3.6	1.0	1.2	2.4	2.1	1.5	1.7	2.7	3.4
Sacroiliac joints	2.2	2.5	3.1	3.7	1.5	1.7	2.6	3.3	1.8	2.1	2.8	3.5
Coronal												
Kidney												
		2.5	3.2	3.8	1.4	1.6	2.6	3.4	1.8	2.1	2.9	3.6
Main portal vein	1.9	2.2	3.0	3.7	1.0	1.3	2.3	3.2	1.5	1.8	2.7	3.4
Total	2.0	2.3	3.1	3.7	1.2	1.4	2.5	3.2	1.7	1.9	2.8	3.5

RD=Reduced dose, FBP=Filtered back projection, ASIR=Adaptive statistical iterative reconstruction, PICCS=Prior image constrained compressed sensing, SD=Standard dose

Table 7

Cumulative focal lesion detection by dose, reconstruction and administration of contrast

	IV contrast				Non contrast				Pooled Results			
Location	**RD- FBP**	**RD-ASIR**	**RD-PICCS**	**SD-FBP**	**RD- FBP**	**RD-ASIR**	**RD-PICCS**	**SD-FBP**	**RD-FBP**	**RD-ASIR**	**RD-PICCS**	**SD-FBP**
Liver	55	53	61	81	2	2	4	13	57	55	65	94
Pancreas	7	6	8	8	0	1	1	0	7	7	9	8
Right Kidney	27	29	32	36	3	2	3	5	30	31	35	41
Left Kidney	48	51	57	66	11	5	18	19	59	56	75	85
Total	137	139	158	191	16	10	26	37	153	149	184	228

RD=Reduced dose, FBP=Filtered back projection, ASIR=Adaptive statistical iterative reconstruction, PICCS=Prior image constrained compressed sensing, SD=Standard dose

Table 8

Cumulative Lesion detection by reader, dose and reconstruction in contrast enhanced CT studies

	Reader 1				Reader 2				Pooled results			
Location	**RD-FBP**	**RD-ASIR**	**RD-PICCS**	**SD-FBP**	**RD-FBP**	**RD-ASIR**	**RD-PICCS**	**SD-FBP**	**RD-FBP**	**RD-ASIR**	**RD-PICCS**	**SD-FBP**
Liver	27	28	30	40	28	25	31	41	55	53	61	81
Pancreas	4	3	5	5	3	3	3	3	7	6	8	8
Right kidney	14	14	14	16	13	15	18	20	27	29	32	36
Left kidney	20	21	29	31	28	30	28	35	48	51	57	66
Total	65	66	78	92	72	73	80	99	137	139	158	191

RD=Reduced dose, FBP=Filtered back projection, ASIR=Adaptive statistical iterative reconstruction, PICCS=Prior image constrained compressed sensing, SD=Standard dose